Disturbance Estimation for the Control of Web Tension in Electrode Calendering

Lisa Wünderlich and Andreas Rauh
Distributed Control in Interconnected Systems, Carl von Ossietzky Universität Oldenburg
Oldenburg, Germany
{lisa.wuenderlich, andreas.rauh}@uni-oldenburg.de

***Abstract*—This study presents a control method for electrode web tension in the context of battery manufacturing, which integrates a state and disturbance observer. This optimization method is applied to the calendering process of electrodes, in order to estimate non-measurable state variables. Desired web tensions before and after calendering are defined as set values, and are obtained by controlling the respective velocity inputs of the calender rolls and nip rolls. For the controller design, the nonlinear dynamic system model is linearized. The results show that this approximation approach for the controller is able to estimate the disturbance of the electrode web tension due to the calendering force. The methodology described in this paper can serve as a baseline approach for state-feedback control and disturbance estimation in the framework of digital twin integration with the aim to optimize process workflows in various battery manufacturing stages.**

***Index Terms*—Tension control, battery manufacturing line, disturbance estimation, disturbance compensation**

I. Introduction

The integration of digital twins in industrial manufacturing lines plays a growing factor in digitalized monitoring of process stages and the whole production line. The EU Horizon project BATTwin "Flexible and scalable digital-twin platform for enhanced production efficiency and yield in battery cell production lines", www.battwin.eu, has the ambitious goal to design, develop, and demonstrate a digital-twin platform for battery cell production lines to strive towards a zero-defect manufacturing solution [4]. Herein, single process digital twins take over the task of monitoring the process and, hence, provide suggestions towards a better quality of the processed product. The calendering process is the last stage within the electrode production. The electrode is compressed between two calendering rolls to obtain the desired thickness and porosity of the active coating, before it can enter the cell assembly process stages. Hereby, the control of the web tension is critical, as too low or high tensions in the calendering stage may cause wrinkles of the web and other defects [6], [13]. These calendering defects propagate to subsequent production stages. For example, defective electrodes can cause misalignment during the stacking of electrode sheets.

State-feedback control and disturbance estimation can be used to estimate non-measurable state variables, and therefore account for missing sensors [3], [9]–[11]. In addition, the estimation results can be used to reduce the effect of external disturbances by an integration of the estimated quantities in a state-feedback control law. Thus, these tools contribute to optimized control workflows within the battery manufacturing line in order to increase the quality of the product.

There exist some literature that investigates web tension control models for disturbance estimation. For example, [2] developed a nonlinear model predictive control scheme to eliminate the tension disturbance in roll-to-roll printed electronics systems. More general, [8] developed an active disturbance rejection control strategy for tension regulation in a web transport system, by using an extended state observer. In another study, a model for web tension control is developed that compensates the periodic disturbances from the rotational frequencies of the roller, by using resonant filters as an additional feedback [12]. However, there is no study that investigates a disturbance control strategy for web tension during calendering, albeit calendering is a critical stage in the production of battery cells.

This study presents a state and disturbance observer-based control method, which is applied for the first time to the process of electrode calendering, to compensate the tension deviation that is caused by the calender rolls. Therefore, this method extends widely applied control strategies, which utilize simple PI and PID controllers. The method makes use of a linearized formulation of the nonlinear physical system equations for the design of the controller. For the simulation of the web tension and velocities, the model from [7] was extended in order to be applicable to the calendering process of electrode production in battery cell manufacturing lines.

Section II introduces the nonlinear system of state equations, which describe the dynamics of the web tension and the roll velocities. In Section III, the system of ordinary differential equations (ODEs) is linearized to obtain a linear state-space representation of the tension model, which is extended by a state-feedback control. Section IV presents the integration of a disturbance observer to compensate the influence of the calendering force on the web tension. The disturbance compensation is simulated for two use-cases. Firstly, all states are assumed to be measurable, and secondly, non-measurable states have to be estimated. The computational results are presented in Section V, followed by a conclusion and outlook in Section VI.

This project has received funding from the European Union's Horizon Europe programme under grant agreement No. 101137954. The authors would like to thank the rest of the BATTwin consortium for supporting this research.

II. Web Tension Model for Calendering Stage

The proposed study extends the model from [7] of web tension between two pairs of nip rolls, by adding a third pair of calendering rolls in between. Two pairs of nip rolls transport the electrode web, while the calendering rolls in the middle use a vertical force to compress the active coating and the current collector. The calendering stage aims at ensuring the optimal thickness and porosity of the electrode. The setting described above is illustrated in Fig. 1.

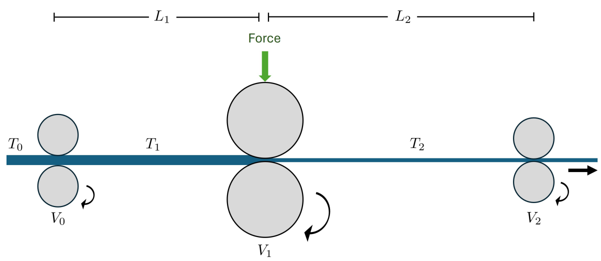

Fig. 1: The proposed setting of the simulated web tension during the calendering stage with two pairs of nip rolls and one pair of calendering rolls in between.

For simplicity, the electrode material is assumed to be a homogeneous linear elastic material, which is characterized by Young's modulus E. Further, L_1 and L_2 denote the distances between the first two pairs of rolls, and the second two pairs of rolls, respectively. The electrode web enters the first pair of rolls with a constant pre-tension T_0. The physical values of interest are the web tensions between the first two pairs of rolls, i.e., the tension T_1 between the first nip rolls and the calendering rolls, and the tension T_2 between the calendering rolls and the following nip rolls. Further, each pair of rolls is assigned their own velocity. These are defined as V_0 for the first pair of nip rolls, which is assumed to be constant, V_1 for the velocity of the calendering rolls, and V_2 for the pair of rolls following the calendering itself. For control, the desired tensions should be reached by determining the velocities V_1 and V_2, which are variable.

The nonlinear system of ODEs

$$\frac{\mathrm{d}T_1}{\mathrm{d}t} = \frac{E}{L_1}\left(V_1 - V_0 - \frac{V_1 T_1}{E} + \frac{V_0 T_0}{E}\right), \tag{1}$$

$$\frac{\mathrm{d}T_2}{\mathrm{d}t} = \frac{E}{L_2}\left(V_2 - V_1 - \frac{V_2 T_2}{E} + \frac{V_1 T_1}{E}\right) + \Delta(F), \tag{2}$$

$$\frac{\mathrm{d}V_1}{\mathrm{d}t} = \frac{1}{T_{\mathrm{Mot}}}\left(V_{1,\mathrm{des}} - V_1\right), \tag{3}$$

$$\frac{\mathrm{d}V_2}{\mathrm{d}t} = \frac{1}{T_{\mathrm{Mot}}}\left(V_{2,\mathrm{des}} - V_2\right), \tag{4}$$

describes the tension and velocity dynamics of the aforementioned setting.

Equations (1) and (2) describe the behaviour of the web tensions before and after passing the calender rolls. Herein, the phenomenological term $\Delta(F)$ describes the change of web tension during thickness reduction by the calendering rolls, which is influenced by physical quantities like calendering force, pressure, or thickness homogeinety. Further, Equations (3) and (4) describe the velocity dynamics of the calender rolls and the following nip rolls, where a delayed speed change is considered in the form of first-order lag dynamics with the temporal parameter T_{Mot} (motor time constant).

III. Linearization and State-Feedback Control

To integrate a state-feedback and disturbance estimation, the nonlinear system of ODEs (1)–(4) is approximated by linearization in a pre-defined operating point. For this, the system of ODEs is rewritten as

$$\dot{\mathbf{x}} = \mathbf{f}(\mathbf{x}, \mathbf{u}), \tag{5}$$

with

$$\mathbf{x} = \begin{pmatrix} T_1 \\ T_2 \\ V_1 \\ V_2 \end{pmatrix} \quad \text{and} \quad \mathbf{u} = \begin{pmatrix} V_{1,\mathrm{des}} \\ V_{2,\mathrm{des}} \end{pmatrix}. \tag{6}$$

A steady-state operating point

$$\mathbf{x}_{\mathrm{O}} = \begin{pmatrix} T_{1,\mathrm{des}} \\ T_{2,\mathrm{des}} \\ V_{1,\mathrm{des}} \\ V_{2,\mathrm{des}} \end{pmatrix} \tag{7}$$

is defined, which is determined by inserting the desired tensions $T_{1,\mathrm{des}}$ and $T_{2,\mathrm{des}}$ into Equations (1) and (2), whereby $\frac{\mathrm{d}T_1}{\mathrm{d}t}$ and $\frac{\mathrm{d}T_2}{dt}$ are set to zero. Solving for V_1 and V_2, the result can be inserted into Equations (3) and (4) to determine $V_{1,\mathrm{des}}$ and $V_{2,\mathrm{des}}$, and ultimatively determine $\mathbf{x}_{\mathrm{O}}$. By defining the Jacobian matrices

$$\mathbf{A} = \left.\frac{\partial \mathbf{f}}{\partial \mathbf{x}}\right|_{\mathbf{x}_{\mathrm{O}}} \quad \text{and} \quad \mathbf{B} = \left.\frac{\partial \mathbf{f}}{\partial \mathbf{u}}\right|_{\mathbf{x}_{\mathrm{O}}}, \tag{8}$$

the nonlinear model equations can be approximated in the linear form

$$\Delta\dot{\mathbf{x}} = \mathbf{A} \cdot \Delta\mathbf{x} + \mathbf{B} \cdot \Delta\mathbf{u}, \tag{9}$$

where $\mathbf{A}$ is the state matrix and $\mathbf{B}$ the input matrix. Here, the vectors $\Delta\mathbf{x}$ and $\Delta\mathbf{u}$ represent deviations from the desired set-point (7) and the respective control input.

Note that the linearized state-space model in Equation (9) is used for the design of the controller, while the nonlinear system is used for the simulation of the physical system. For state-feedback control design, an optimal gain matrix $\mathbf{K}$ is calculated by minimizing the integral quadratic cost function

$$\begin{aligned} J = \int_0^\infty \Bigg(& \underbrace{(T_1 - T_{1,\mathrm{des}})^2 + (T_2 - T_{2,\mathrm{des}})^2}_{\Delta\mathbf{x}^T\mathbf{Q}\Delta\mathbf{x}} \\ & + \underbrace{\alpha(V_{1,\mathrm{des}}^2 + V_{2,\mathrm{des}}^2)}_{\Delta\mathbf{u}^T\mathbf{R}\Delta\mathbf{u}} \Bigg) \, \mathrm{d}t. \end{aligned} \tag{10}$$

Herein, the weighing matrices $\mathbf{Q}$ and $\mathbf{R}$ for the costs of deviations from the desired operating state and the corresponding control values are expressed as

$$\mathbf{Q} = \begin{pmatrix} 1 & 0 & 0 & 0 \\ 0 & 1 & 0 & 0 \\ 0 & 0 & 0 & 0 \\ 0 & 0 & 0 & 0 \end{pmatrix} \quad \text{and} \quad \mathbf{R} = \begin{pmatrix} \alpha & 0 \\ 0 & \alpha \end{pmatrix}, \tag{11}$$

where the parameter α allows for adjusting the control effort.

The gain matrix $\mathbf{K} = \mathbf{R} \cdot \mathbf{B}^T \cdot \mathbf{P}$ is obtained from the solution $\mathbf{P}$ of the respective Riccati equation for the linear quadratic regulator problem, i.e., the above minimization problem. Then, the state-feedback control input $\Delta\mathbf{u} = -\mathbf{K} \cdot \Delta\mathbf{x}$ for the linearized problem can be obtained. Thus, the state-feedback control input for the nonlinear problem is given by

$$\mathbf{u} = \mathbf{u}_{\mathrm{O}} + \Delta\mathbf{u} = \mathbf{u}_{\mathrm{O}} - \mathbf{K} \cdot (\mathbf{x} - \mathbf{x}_{\mathrm{O}}). \tag{12}$$

The respective block diagram for state-feedback can be seen in Fig. 2. Within the above described system, an increase of the force of the calendering rolls reduces the thickness of the electrode web, thereby also reducing the tension T_2. Therefore, the force acts as a disturbance to the system.

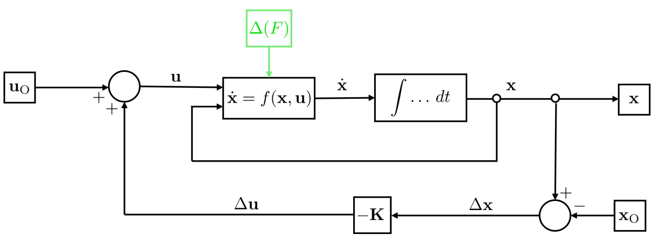

Fig. 2: Block diagram of the state-feedback control model. The phenomenological term $\Delta(F)$ originates from the calendering force and acts as a disturbance input to the system model.

IV. Disturbance Estimation

The implementation of a disturbance estimator for the state-space system aims to compensate the disturbance generated by the calendering force. For this, the state-space representation in Equation (9) is extended to include a disturbance variable z according to

$$\begin{pmatrix} \Delta\dot{\mathbf{x}} \\ \dot{z} \end{pmatrix} = \underbrace{\begin{pmatrix} \mathbf{A} & \mathbf{e} \\ \mathbf{0}^T & 0 \end{pmatrix}}_{\tilde{\mathbf{A}}} \cdot \underbrace{\begin{pmatrix} \Delta\mathbf{x} \\ z \end{pmatrix}}_{\tilde{\mathbf{x}}} + \underbrace{\begin{pmatrix} \mathbf{B} \\ 0 \end{pmatrix}}_{\tilde{\mathbf{B}}} \cdot \Delta\mathbf{u}. \tag{13}$$

In this model, the assumption of an integrator disturbance model $\dot{z} = 0$ is justified by the slow variation of this quantity. Its actual value is adjusted by taking into consideration measured outputs with the help of a combined state and disturbance observer.

These measurements are related to the state vector via the output equation

$$\mathbf{y} = \underbrace{\begin{pmatrix} \mathbf{C} & 0 \end{pmatrix}}_{\tilde{\mathbf{C}}} \cdot \begin{pmatrix} \Delta\mathbf{x} \\ z \end{pmatrix}. \tag{14}$$

Equation (14) indicates that the disturbance is not measurable. For the computational study, two use-cases are considered, which are defined as follows:

- In use-case 1, it is assumed that all states are measurable outputs. In this regard, the output matrix reads

$$\mathbf{C} = \begin{pmatrix} 1 & 0 & 0 & 0 \\ 0 & 1 & 0 & 0 \\ 0 & 0 & 1 & 0 \\ 0 & 0 & 0 & 1 \end{pmatrix}. \tag{15}$$

- In use-case 2, it is assumed that only the difference between the web tensions T_1 and T_2, and the velocity V_1 of the calendering rolls are measurable, which means that the state-output matrix reads

$$\mathbf{C} = \begin{pmatrix} -1 & 1 & 0 & 0 \\ 0 & 0 & 1 & 0 \end{pmatrix}. \tag{16}$$

In both cases, it is required that the observability matrix

$$\mathbf{Q}_{\mathrm{obs}} = \begin{pmatrix} \tilde{\mathbf{C}} \\ \tilde{\mathbf{C}}\tilde{\mathbf{A}} \\ \vdots \\ \tilde{\mathbf{C}}\tilde{\mathbf{A}}^n \end{pmatrix} \tag{17}$$

has the full rank $n+1$, corresponding to the dimension of the augmented state vector $\tilde{\mathbf{x}}$ with $\mathbf{x} \in \mathbb{R}^n$. If this criterion is fulfilled, then the disturbance input and all non-measured state variables can be estimated (at least in the vicinity of the linearization point) by using the observer

$$\dot{\hat{\tilde{\mathbf{x}}}} = \tilde{\mathbf{A}} \cdot \hat{\tilde{\mathbf{x}}} + \tilde{\mathbf{B}} \cdot \Delta\mathbf{u} + \mathbf{H} \cdot (\mathbf{y}_{\mathrm{m}} - \hat{\mathbf{y}}). \tag{18}$$

Herein, $\hat{\mathbf{y}} = \tilde{\mathbf{C}} \cdot \hat{\tilde{\mathbf{x}}}$ is the estimated output, $\mathbf{y}_{\mathrm{m}}$ is the measured output, and $\mathbf{H}$ is the observer gain matrix, which is calculated by using the method of pole placement. Hereby, the state variable whose measurement is most likely to be of interest is given greater weighting.

Finally, the estimated disturbance $\hat{z}$ is multiplied by the correction factor

$$\mathbf{G} = \begin{pmatrix} 0 \\ \dfrac{-L_2}{E - T_{2,\mathrm{des}}} \end{pmatrix} \tag{19}$$

to obtain the corrected control signal. The vector $\mathbf{G}$ follows from comparing Equation (2) for the nominal input V_2 without disturbance and the estimated input $\tilde{V}_2$ with disturbance, in particular from the relation

$$V_2 - \frac{V_2 T_2}{E} = \tilde{V}_2 - \frac{\tilde{V}_2 T_2}{E} + \frac{E}{L_2}\Delta(F), \tag{20}$$

in which the terms V_1 cancels out. For the nominal input $V_{2,\mathrm{des}}$ and the estimated input $\tilde{V}_{2,\mathrm{des}}$, this results in the relationship

$$V_{2,\mathrm{des}} = \frac{-L_2}{E - T_{2,\mathrm{des}}} \cdot \Delta(F) + \tilde{V}_{2,\mathrm{des}}. \tag{21}$$

Thus, the corrected control signal is added onto the state-feedback control to obtain the overall control signal

$$\Delta\mathbf{u}_{\mathrm{control}} = \mathbf{G} \cdot \hat{z} + \Delta\mathbf{u} = \mathbf{G} \cdot \hat{z} - \mathbf{K} \cdot \Delta\mathbf{x}. \tag{22}$$

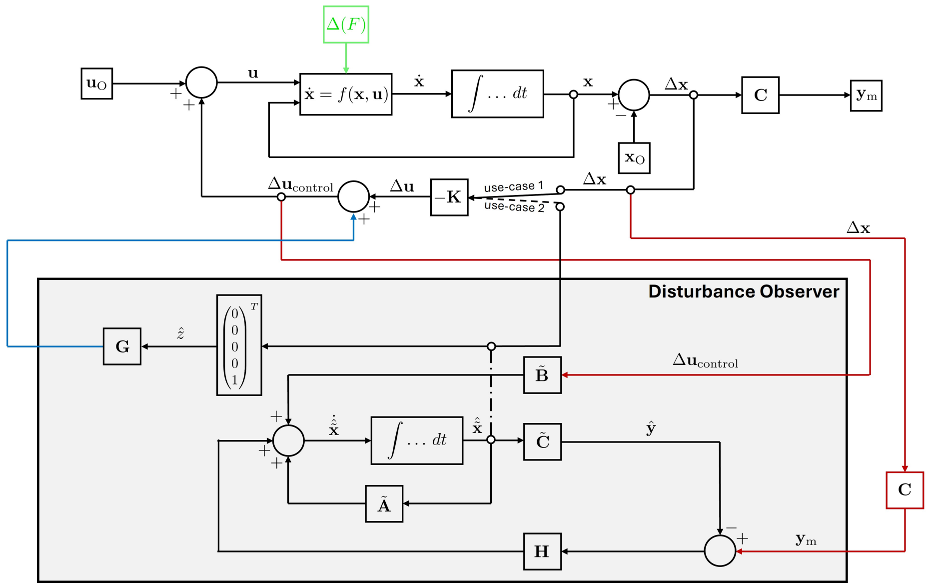

Fig. 3: Block diagram of the disturbance estimation model. The overall control signal $\Delta \mathbf{u}_{\mathrm{control}}$ and the measured output $\mathbf{y}_{\mathrm{m}}$ are the two input signals for the disturbance observer, indicated with a red line, and the corrected control signal $\mathbf{G} \cdot \hat{z}$ is the output of the disturbance observer, indicated with a blue line.

The integration of the disturbance observer into the state-feedback controller is illustrated as a block diagram in Fig. 3. Besides providing the estimate $\hat{z}$ this observer is used to reconstruct information about $\Delta \mathbf{x}$ if the state is not fully measurable and to perform a model-based low-pass filtering of the measurements before using them in the state-feedback.

V. Numerical Simulation Results

For the numerical validation study, a total time of 400 s of electrode web tension control during calendering is simulated using Matlab/Simulink. Within this time frame, the first part of the simulation considers the calender rolls to be inactive, which means that there is no disturbance to the system coming from the applied force of the calender rolls. During this first part, the web tensions and velocities are reaching their steady state. After the steady state has been reached, the calender rolls start to compress the electrode web. This is expressed in a first approach by a stepwise decrease of the phenomenological disturbance term $\Delta(F)$ to a predefined value, which is then held constant for the rest of the simulation time. More precisely, the disturbance influence is defined by

$$\Delta(F)(t) = \begin{cases} 0 & t < 200, \\ -100 & t \geq 200. \end{cases} \tag{23}$$

In a second approach, the initiation of the disturbance from the calender force is expressed by a smoothed form of Equation (23), given by

$$\Delta(F)(t) = -\frac{100}{1 + \exp\left(-(t - 200)\right)}, \tag{24}$$

which is more closely resembling the behaviour of the activation of the calender rolls. The remaining model parameters for all simulations are given in Table I.

TABLE I: Model parameter values and their respective units used for the simulation of electrode web tension control.

Parameter	Value	Unit
E	5	GPa
L_1	2.5	m
L_2	2.5	m
V_0	800	m min^{-1}
T_0	500	N m^{-1}
T_{Mot}	10	min^{-1}
$T_{1,\mathrm{des}}$	500	N m^{-1}
$T_{2,\mathrm{des}}$	510	N m^{-1}

Fig. 4 summarizes the results from use-case 1, where all states are measurable. The top row of Fig. 4 depicts the temporal behaviour of the web tension T_2 after reaching steady state. On the left, the influence of the calender force is initiated through a stepwise decrease of $\Delta(F)$ at 200 s, see Fig. 4a. This is indicated by a drop of the tension T_2 from the desired web tension $T_{2,\mathrm{des}} = 510$ N m^{-1} to approximately 509.68 N m^{-1}, for the case that no disturbance observer-based error compensation is performed.

However, it can be clearly seen that the inclusion of the disturbance observer together with the presented compensation method is able to reduce the influence of $\Delta(F)$ after 200 s. It takes around 50 s for the controller to correct the tension to a value of $T_2 = 509.95$ N m^{-1} which is close enough to the desired value. In contrast, without the disturbance observer-based compensation, the tension drop remains constant over the complete rest of the simulation time, as depicted in Fig. 4a, indicating a permanent deviation of web tension due to the calender force. Thus, the disturbance observer is able to compensate around 84% of the tension deviation.

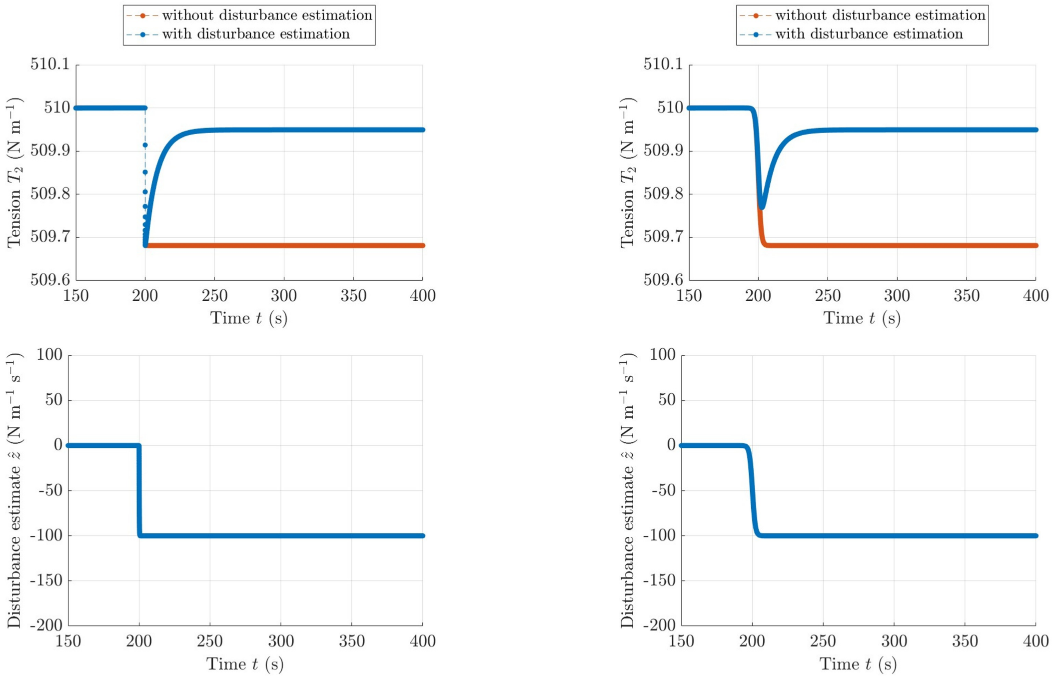

(a) Stepwise disturbance input.

(b) Smooth disturbance input.

Fig. 4: In use-case 1, it is assumed that all state variables are measurable. The top row shows the temporal behaviour of the web tension T_2 with and without compensation through a disturbance observer. The lower row shows the temporal behaviour of the estimated disturbance $\hat{z}$ when using a disturbance observer.

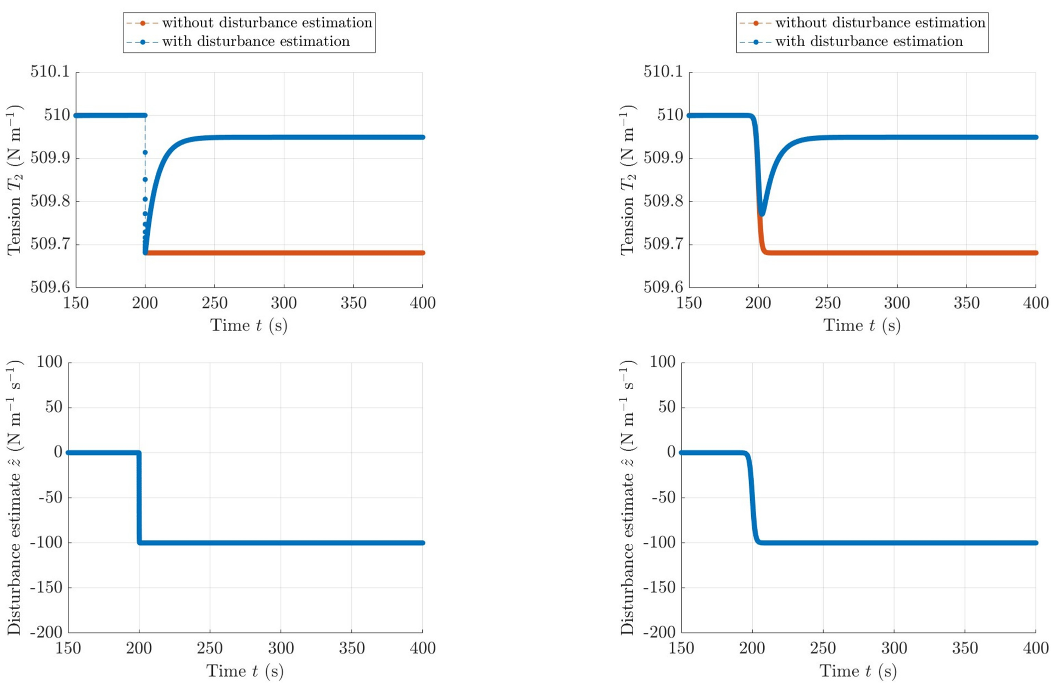

(a) Stepwise disturbance input

(b) Smoothed disturbance input

Fig. 5: For use-case 2, the non-measurable state variables are estimated by the disturbance observer and used to implement the state-feedback control law. The results are similar to use-case 1 in Fig. 4.

For the smooth disturbance input, the observer has already started compensation before the tension reaches the lowest value, see Fig. 4b. In accordance to these findings, the disturbance observer is able to correctly estimate the disturbance $\Delta(F)$ from the measured states, as seen in the lower row of Fig. 4. Here, the plot for the estimated disturbance $\hat{z}$ is shown for both the stepwise disturbance input (Fig. 4a) and for the smoothed input (Fig. 4b).

Fig. 5 depicts the results from use-case 2, where only the difference of the web tensions and the velocity of the calender rolls are measurable states and, therefore, the estimated state vector $\hat{\hat{\mathbf{x}}}$ obtained by the disturbance observer is used for the state-feedback control. This significantly reduces the hardware requirements, as the measured outputs can be replaced by the estimated values. Here, without loss of accuracy, the disturbance observer is still able to compensate the disturbance, and also estimate the disturbance correctly, for both the stepwise and the smooth disturbance input.

VI. Conclusions and Outlook on Future Work

This study presents a control-oriented modeling approach for the web tension in the calendering stage of battery cell production. This model is extended by a state and disturbance observer to compensate the tension reduction originating from the calender force. For this, linearized system equations are used for controller design, while the physical system output is simulated using the nonlinear system equations. The numerical results in this study are purely simulation-based. The model output can be replaced by real measured data of web tension and roll velocities during operation of electrode calendering for real-time application. The results show that the proposed control strategy is able to estimate and compensate both stepwise and smoothed disturbance inputs resulting from variations of the calendering force, even though not all states of the system are known. Hereby, a model limitation is the phenomenological modeling of the disturbance input for the tension reduction.

The proposed strategy of disturbance compensation control can be integrated as a digital twin to optimize process workflows of battery cell manufacturing stages, by estimating non-measurable states and disturbances. Deviations from desired electrode web tensions during the calendering stage may lead to wrinkles and other defects, that further propagate to subsequent process stages. These external disturbances can be estimated by the method proposed in this study, which can serve as a baseline approach for state-feedback control and disturbance estimation.

In future work, the model can be extended to estimate other unknown variables, e.g., the pre-tension T_0 of the electrode web, which will undergo unknown fluctuations during roller exchange. This is especially relevant for online testing of the electrode web before calendering, when samples are taken in the frame of inline quality checks. Further, the proposed control strategy can be extended to account for uncertainty identification schemes [14]. Extrapolation of future web tension behaviour is possible by exploiting the analytical formulation of the system equations, so that model predictive control strategies can be included [1], [5].

References

[1] E. Camacho and C. Alba. *Model Predictive Control*. Advanced Textbooks in Control and Signal Processing. Springer London, 2013.

[2] W. Chen, X. Sun, W. Chen, G. Xie, S. Chen, and J. Wang. Nonlinear web tension control of a roll-to-roll printed electronics system. *Precision Engineering*, 76:88–94, 2022.

[3] W.-H. Chen, J. Yang, L. Guo, and S. Li. Disturbance-observer-based control and related methods—an overview. *IEEE Transactions on Industrial Electronics*, 63(2):1083–1095, 2016.

[4] O. Demir, M. Colledani, G. Horváth, D. Marzogui, and K. Giakoumi. A Novel Zero-Defect Manufacturing Approach for Defect Reduction in Battery Production. *Procedia CIRP*, 134:1167–1172, 01 2025.

[5] W. Frenkel, J. Kersten, H. Aschemann, and A. Rauh. Model predictive control as an industrially applicable approach for power control of solid oxide fuel cells. In *2021 25th International Conference on Methods and Models in Automation and Robotics (MMAR)*, pages 251–256, 2021.

[6] Z. Fu. The effect of web tension on calendering wrinkles and corrugations of coated foils. In *Metal Forming 2024*, Materials Research Proceedings, pages 305–319. Materials Research Forum LLC, 2024.

[7] K. P. Grenfell. Tension control paper-making and converting machinery. *IEEE Transactions on Applications and Industry*, 83(73):234–240, 1964.

[8] Y. Hou, Z. Gao, F. Jiang, and B. T. Boulter. Active disturbance rejection control for web tension regulation. In *Proceedings of the 40th IEEE Conference on Decision and Control (Cat. No.01CH37228)*, pages 4974–4979. IEEE, 2001.

[9] C. Johnson. Optimal control of the linear regulator with constant disturbances. *IEEE Transactions on Automatic Control*, 13(4):416–421, 1968.

[10] C. Johnson. Accomodation of external disturbances in linear regulator and servomechanism problems. *IEEE Transactions on Automatic Control*, 16(6):635–644, 1971.

[11] C. D. Johnson. Real-time disturbance-observers; origin and evolution of the idea part 1: The early years. In *2008 40th Southeastern Symposium on System Theory (SSST)*, pages 88–91, 2008.

[12] K. Seki, T. Kikuchi, and M. Iwasaki. Tension controller design considering periodic disturbance suppression in roll-to-roll web handling systems. *IEEJ Journal of Industry Applications*, 9(1):36–42, 2020.

[13] A.-K. Wurba, J. Klemens, D. Mayer, C. Reusch, L. Altmann, O. Leonet, J. A. Blázquez, I. Boyano, E. Ayerbe, P. Scharfer, W. Schabel, and J. Fleischer. Methodology for the characterization and understanding of longitudinal wrinkling during calendering of lithium-ion and sodium-ion battery electrodes. *Procedia CIRP*, 120:314–319, 2023.

[14] L. Wünderlich and A. Rauh. Uncertainty quantification of identified parameters in battery cell manufacturing. In *2025 29th International Conference on Methods and Models in Automation and Robotics (MMAR)*, pages 29–34, 2025.